

Exploring Spin-3/2 Dark Matter with Effective Higgs Couplings

Chia-Feng Chang¹, Xiao-Gang He^{1,2,3}, and Jusak Tandean^{1,3}

¹*Department of Physics and Center for Theoretical Sciences, National Taiwan University,
No. 1, Sec. 4, Roosevelt Rd., Taipei 106, Taiwan*

²*INPAC, Department of Physics and Astronomy, Shanghai Jiao Tong University,
800 Dongchuan Rd., Minhang, Shanghai 200240, China*

³*Physics Division, National Center for Theoretical Sciences,
No. 101, Sec. 2, Kuang Fu Rd., Hsinchu 300, Taiwan*

Abstract

We study an economical model of weakly-interacting massive particle dark matter (DM) which has spin 3/2 and interacts with the 125-GeV Higgs boson via effective scalar and pseudoscalar operators. We apply constraints on the model from the relic density data, LHC measurements of the Higgs boson, and direct and indirect searches for DM, taking into account the effective nature of the DM-Higgs couplings. We find that this DM is currently viable in most of the mass region from about 58 GeV to 2.3 TeV and will be probed more stringently by ongoing and upcoming experiments. Nevertheless, the presence of the DM-Higgs pseudoscalar coupling could make parts of the model parameter space elusive from future tests. This scenario is quite similar to its more popular spin-1/2 counterpart.

I. INTRODUCTION

Various astronomical and cosmological observations over the past several decades have led to the wide acceptance that dark matter (DM) exists in our Universe, making up about 26% of its energy budget [1]. Despite the evidence, however, the identity of the basic constituents of the bulk of DM has so far remained a mystery. Since it cannot be accommodated by the standard model (SM) of particle physics, it is of much interest to look into different possibilities beyond the SM which can offer good candidates for DM.

Here we consider an economical scenario of DM which is of the popular weakly interacting massive particle (WIMP) type and has spin $3/2$. Such DM is a viable alternative, although it has gained less attention than WIMP candidates with spin 0, $1/2$, or 1 in the literature (*e.g.*, [2–8]). Among analyses on spin- $3/2$ DM in recent years [9–12] are those that have examined its potential interactions with SM members via effective nonrenormalizable operators without explicitly involving other new particles [9–11]. In the following, we adopt this line of investigation and focus specifically on the effective couplings of the DM to the standard Higgs doublet.

This study is partly motivated by the null findings of the LUX [13] and PandaX-II [14] direct detection experiments last year, which translate into the most stringent upper-bounds to date on the cross section of spin-independent elastic WIMP-nucleon scattering for WIMP masses between 4 GeV and 100 TeV. These results imply major constraints on WIMP DM models, especially the simplest Higgs-portal ones, which are also subject to restrictions from quests at the LHC [15, 16] for decays of the 125-GeV Higgs boson into final states which would signal the occurrence of new physics. In particular, as we demonstrated in Ref. [11], spin- $3/2$ DM that links up with the Higgs solely via an effective scalar operator is ruled out by the combination of direct search and LHC data, except if the DM has a mass within a very small region slightly below one half of the Higgs mass. However, as also elaborated in Ref. [11], if the model is enlarged somewhat with another Higgs doublet, one could regain a good number of the eliminated masses. In the present paper, we explore instead a different possibility in which we keep the minimal particle content of the SM plus the spin- $3/2$ DM and the DM-Higgs interactions arise not only from the effective scalar operator, but also from an effective pseudoscalar operator. This modification turns out to provide the model with the freedom to evade the preceding limitations over much of mass region of concern. Specifically, with the appropriate admixture of contributions from the scalar and pseudoscalar couplings, the model can reproduce the observed DM relic abundance and simultaneously yield DM-nucleon cross-sections which are low enough to allow for the recovery of sizable parts of the excluded parameter space. We will also look at a complementary probe on the model from indirect searches for DM.

In Sec. II, we describe the model and address the constraints on it from Higgs measurements and DM direct searches. Since we assume that the interactions of the spin- $3/2$ DM with the Higgs are induced by effective nonrenormalizable operators in the absence of other new particles, we also take into account the restriction due to the limited extent of the reliability of the effective-theory approximation. Subsequently, we discuss examples of the viable parameter space of the model. In Sec. III, we make some comparison with the Higgs-portal spin- $1/2$ DM. In addition, we briefly consider how DM indirect searches can offer complementary tests on these scenarios. We give our conclusions in Sec. IV.

II. HIGGS-PORTAL SPIN-3/2 DARK MATTER

The WIMP DM of interest is described by a Rarita-Schwinger field [17], denoted hereafter by a Dirac four-spinor Ψ_ν with a vector index ν . Its free Lagrangian can be expressed as

$$\mathcal{L}_0 = \overline{\Psi}_\kappa L^{\kappa\nu} \Psi_\nu, \quad (1)$$

where [18]¹

$$L^{\kappa\nu} = -(i\cancel{\partial} - \mu_\Psi)g^{\kappa\nu} - \gamma^\kappa(i\cancel{\partial} + \mu_\Psi)\gamma^\nu + i\gamma^\kappa\partial^\nu + i\gamma^\nu\partial^\kappa. \quad (2)$$

From \mathcal{L}_0 follows the equation of motion $L^{\kappa\nu}\Psi_\nu = 0$ which implies²

$$\gamma^\nu\Psi_\nu = 0, \quad \partial^\nu\Psi_\nu = 0, \quad (i\cancel{\partial} - \mu_\Psi)\Psi_\nu = 0. \quad (3)$$

The sums over polarizations, ς , of Ψ and its antiparticle are [19]

$$\begin{aligned} \sum_{\varsigma=-3/2}^{3/2} u_{p,\varsigma}^\kappa \bar{u}_{p,\varsigma}^\nu &= (\not{p} + \mu_\Psi) \left(-\mathcal{G}^{\kappa\nu}(p) + \frac{\gamma_\rho \gamma_\omega}{3} \mathcal{G}^{\rho\kappa}(p) \mathcal{G}^{\omega\nu}(p) \right), \\ \sum_{\varsigma=-3/2}^{3/2} v_{p,\varsigma}^\kappa \bar{v}_{p,\varsigma}^\nu &= (\not{p} - \mu_\Psi) \left(-\mathcal{G}^{\kappa\nu}(p) + \frac{\gamma_\rho \gamma_\omega}{3} \mathcal{G}^{\rho\kappa}(p) \mathcal{G}^{\omega\nu}(p) \right) \end{aligned} \quad (4)$$

where $\mathcal{G}^{\kappa\nu}(p) = g^{\kappa\nu} - p^\kappa p^\nu / p^2$ and $p^2 = \mu_\Psi^2$.

We assume that the DM candidate is stable due to an unbroken Z_2 symmetry under which $\Psi_\nu \rightarrow -\Psi_\nu$ and SM fields are not affected. Furthermore, the lowest-order Higgs-portal interactions arise from dimension-five operators involving the Higgs doublet H given by [9]

$$\mathcal{L}_{\text{int}} = \left(\frac{\overline{\Psi}_\nu \Psi^\nu}{\Lambda} + \frac{i\overline{\Psi}_\nu \gamma_5 \Psi^\nu}{\Lambda_5} \right) H^\dagger H, \quad (5)$$

where Λ and Λ_5 are real constants which in general depend on the couplings and masses characterizing the underlying heavy physics. After electroweak symmetry breaking, we have

$$\mathcal{L} = \mathcal{L}_0 + \mathcal{L}_{\text{int}} \supset \overline{\Psi}_\nu \left(\mu_\Psi + \frac{v^2}{2\Lambda} + \frac{i\gamma_5 v^2}{2\Lambda_5} \right) \Psi^\nu + \overline{\Psi}_\nu \left(\frac{1}{\Lambda} + \frac{i\gamma_5}{\Lambda_5} \right) \Psi^\nu \left(hv + \frac{h^2}{2} \right), \quad (6)$$

where h refers to the physical Higgs boson and $v \simeq 246$ GeV is the vacuum expectation value (VEV) of H . Because of the Λ_5 contribution, Ψ^ν in Eq. (6) is not yet a mass eigenstate. Therefore, we need to perform the transformation $\Psi_\nu \rightarrow e^{-i\gamma_5 \theta/2} \Psi_\nu$, so that we arrive at

$$\mathcal{L} \supset m_\Psi \overline{\Psi}_\nu \Psi^\nu + \overline{\Psi}_\nu \left(\frac{1}{\Lambda} + \frac{i\gamma_5}{\Lambda_5} \right) e^{-i\gamma_5 \theta} \Psi^\nu \left(hv + \frac{h^2}{2} \right), \quad (7)$$

¹ It is simple to obtain $L^{\kappa\nu} = \{\cancel{\partial} - m_\Psi, [\gamma^\kappa, \gamma^\nu]\}/4 = \epsilon^{\kappa\rho\omega\nu} \gamma_5 \gamma_\rho \partial_\omega - [\gamma^\kappa, \gamma^\nu] m_\Psi/2$, with $\epsilon_{0123} = +1$. These alternative formulas for $L^{\kappa\nu}$ are also employed in the literature [19].

² More generally [18], $L^{\kappa\nu} = -(i\cancel{\partial} - \mu_\Psi)g^{\kappa\nu} - iA\gamma^\kappa\partial^\nu - iA^*\gamma^\nu\partial^\kappa - \gamma^\kappa(iB\cancel{\partial} + C\mu_\Psi)\gamma^\nu$, where A ($\neq -1/2$) can be complex, $B = 1/2 + \text{Re } A + 3|A|^2/2$, and $C = 1 + 3\text{Re } A + 3|A|^2$. Thus $A = -1$ leads to Eq. (2). It is straightforward to check that the relations in Eq. (3) are independent of A . Also, the conditions $\gamma^\nu\Psi_\nu = \partial^\nu\Psi_\nu = 0$ imply that quantities such as cross sections for Ψ and $\bar{\Psi}$ being exclusively on-shell do not depend on A .

where now Ψ^ν is the mass eigenstate with mass

$$m_\Psi = \sqrt{\left(\mu_\Psi + \frac{v^2}{2\Lambda}\right)^2 + \frac{v^4}{4\Lambda_5^2}}, \quad (8)$$

which is related to θ by

$$\cos \theta = \frac{\mu_\Psi}{m_\Psi} + \frac{v^2}{2\Lambda m_\Psi}, \quad \sin \theta = \frac{v^2}{2\Lambda_5 m_\Psi}. \quad (9)$$

Consequently, m_Ψ replaces μ_Ψ in Eqs. (3) and (4). Moreover, the Ψ - h interaction parts in Eq. (7) can be rewritten as

$$\mathcal{L} \supset \bar{\Psi}_\nu (\lambda_S + i\gamma_5 \lambda_P) \Psi^\nu \left(h + \frac{h^2}{2v} \right), \quad (10)$$

with

$$\lambda_S = \frac{v \cos \theta}{\Lambda} + \frac{v \sin \theta}{\Lambda_5}, \quad \lambda_P = \frac{v \cos \theta}{\Lambda_5} - \frac{v \sin \theta}{\Lambda}. \quad (11)$$

There are a couple of special cases worth mentioning. If the Λ_5 term in Eq. (5) is absent, corresponding to $\Lambda_5 \rightarrow \infty$ and hence $\theta \rightarrow 0$, then $\lambda_S = v/\Lambda$ and $\lambda_P = 0$, which is the case already treated in Ref. [11]. If there is no scalar coupling in Eq. (5), due to $\Lambda \rightarrow \infty$, then

$$m_\Psi = \sqrt{\mu_\Psi^2 + \frac{v^4}{4\Lambda_5^2}}, \quad \lambda_S = \frac{v^3}{2\Lambda_5^2 m_\Psi}, \quad \lambda_P = \frac{\mu_\Psi v}{\Lambda_5 m_\Psi}.$$

We see that $1/\Lambda_5 \neq 0$ always yields a contribution to λ_S provided that $\tan \theta \neq -\Lambda_5/\Lambda$. More generally, since we have taken μ_Ψ , Λ , and Λ_5 to be free parameters, so are m_Ψ and $\lambda_{S,P}$.

The couplings $\lambda_{S,P}$ are responsible for the DM relic density, which results from $\bar{\Psi}\Psi$ annihilation into SM particles, mainly via the Higgs-mediated process $\bar{\Psi}\Psi \rightarrow h^* \rightarrow X_{\text{SM}}$. If the center-of-mass energy \sqrt{s} of the $\bar{\Psi}\Psi$ pair exceeds twice the Higgs mass, m_h , the channel $\bar{\Psi}\Psi \rightarrow hh$, due to contact and h -exchange diagrams, has to be computed as well.³ Thus, the cross section σ_{ann} of DM annihilation is given by

$$\begin{aligned} \sigma_{\text{ann}} &= \sigma(\bar{\Psi}\Psi \rightarrow h^* \rightarrow X_{\text{SM}}) + \sigma(\bar{\Psi}\Psi \rightarrow hh), \\ \sigma(\bar{\Psi}\Psi \rightarrow h^* \rightarrow X_{\text{SM}}) &= \frac{(\eta_S \lambda_S^2 + \eta_P \lambda_P^2) s^{5/2} \sum_i \Gamma(\tilde{h} \rightarrow X_{i,\text{SM}})}{72 \beta_\Psi m_\Psi^4 [(s - m_h^2)^2 + \Gamma_h^2 m_h^2]}, \quad X_{i,\text{SM}} \neq hh, \\ \sigma(\bar{\Psi}\Psi \rightarrow hh) &= \frac{\beta_h (\eta_S \lambda_S^2 + \eta_P \lambda_P^2) s^2}{2304 \beta_\Psi \pi m_\Psi^4 v^2} (\mathcal{R}_{hh}^2 + \mathcal{I}_{hh}^2), \end{aligned} \quad (12)$$

³ We have dropped contributions to $\bar{\Psi}\Psi \rightarrow hh$ from t - and u -channel Ψ -mediated diagrams because they are of a higher order in $\lambda_{S,P}$ and of the same order as the potential contributions of next-to-leading effective operators not included in Eq. (10).

where

$$\begin{aligned}\beta_x &= \sqrt{1 - \frac{4m_x^2}{s}}, & \eta_s &= \frac{5\beta_\Psi^2 - 6\beta_\Psi^4 + 9\beta_\Psi^6}{8}, & \eta_p &= \frac{9 - 6\beta_\Psi^2 + 5\beta_\Psi^4}{8}, \\ \mathcal{R}_{hh} &= 1 + \frac{3m_h^2(s - m_h^2)}{(s - m_h^2)^2 + \Gamma_h^2 m_h^2}, & \mathcal{I}_{hh} &= \frac{3\Gamma_h m_h^3 v^2}{(s - m_h^2)^2 + \Gamma_h^2 m_h^2}.\end{aligned}\quad (13)$$

Once $\lambda_{s,p}$ have been extracted from the observed relic density, as outlined in Ref. [11], their values can be tested with various constraints.

If $m_\Psi < m_h/2$, the invisible channel $h \rightarrow \bar{\Psi}\Psi$ is open. We calculate its rate to be

$$\Gamma(h \rightarrow \bar{\Psi}\Psi) = \frac{m_h}{8\pi} \frac{\lambda_s^2(1 - 4\mathcal{R}_\Psi^2)(1 - 6\mathcal{R}_\Psi^2 + 18\mathcal{R}_\Psi^4) + \lambda_p^2(1 - 2\mathcal{R}_\Psi^2 + 10\mathcal{R}_\Psi^4)}{9\mathcal{R}_\Psi^4} \sqrt{1 - 4\mathcal{R}_\Psi^2}, \quad (14)$$

where $\mathcal{R}_f = m_f/m_h$. The LHC Higgs experiments can probe $\lambda_{s,p}$ for $m_\Psi < m_h/2$ via this decay mode. According to the joint analysis by the ATLAS and CMS Collaborations on their measurements [16], the branching fraction of Higgs decay into channels beyond the SM is $\mathcal{B}_{\text{BSM}}^{\text{exp}} = 0.00^{+0.16}$, which can be interpreted as capping the branching fraction of $h \rightarrow \bar{\Psi}\Psi$. As a consequence, we may impose

$$\mathcal{B}(h \rightarrow \bar{\Psi}\Psi) = \frac{\Gamma(h \rightarrow \bar{\Psi}\Psi)}{\Gamma_h} < 0.16, \quad (15)$$

where $\Gamma_h = \Gamma_h^{\text{SM}} + \Gamma(h \rightarrow \bar{\Psi}\Psi)$ is the Higgs' total width, which also enters the formulas in the last paragraph. In numerical work, we set $m_h = 125.1 \text{ GeV}$, based on the current data [20], and correspondingly the SM width $\Gamma_h^{\text{SM}} = 4.08 \text{ MeV}$ [21].

Another important test is available from direct detection experiments, which look for recoil signals of nuclei due to the DM scattering off a nucleon, N , nonrelativistically at momentum transfers small relative to the nucleon mass, m_N . The relevant process is $\Psi N \rightarrow \Psi N$, which is mediated by the Higgs in the t channel. Its cross section in the nonrelativistic limit is

$$\sigma_{\text{el}}^N = \frac{g_{NNh}^2 m_\Psi^2 m_N^2}{\pi (m_\Psi + m_N)^2 m_h^4} \left[\lambda_s^2 + \frac{5\lambda_p^2 m_N^2 v_{\Psi,\text{lab}}^2}{18(m_\Psi + m_N)^2} \right], \quad (16)$$

where g_{NNh} denotes the effective Higgs-nucleon coupling defined by $\mathcal{L}_{NNh} = -g_{NNh} h \bar{N}N$ and $v_{\Psi,\text{lab}}$ is the speed of the initial Ψ in the laboratory frame. Numerically, we adopt $g_{NNh} = 0.0011$ following Ref. [3] and $v_{\Psi,\text{lab}} = 300 \text{ km/s} = 10^{-3}$ [1] relative to the speed of light. The strongest restraints on σ_{el}^N to date for $m_\Psi \gtrsim 5 \text{ GeV}$ are supplied by LUX [13] and PandaX-II [14].

In Eq. (16), the $v_{\Psi,\text{lab}}^2$ factor clearly causes huge suppression in the relative size of the λ_p and λ_s contributions to σ_{el}^N . On the other hand, from Eq. (12) we see that in the annihilation rate $\sigma_{\text{ann}} v_{\text{rel}}$, where v_{rel} is the relative speed of $\bar{\Psi}$ and Ψ in their center of mass, the λ_s term is suppressed by v_{rel}^2 whereas the λ_p term is not, as $\beta_\Psi \sim v_{\text{rel}}/2$ in the nonrelativistic limit. This suggests that there may be admixtures of λ_s and λ_p contributions to σ_{ann} and σ_{el}^N such that the various pertinent requirements can be fulfilled. Our numerical calculations below demonstrate that this is indeed the case.

Since we have $\lambda_{S,P}$ as the free parameters besides m_Ψ , it is convenient to express

$$\begin{aligned}\lambda_S &= \lambda_{\Psi h} \cos \xi, & \lambda_P &= \lambda_{\Psi h} \sin \xi, \\ \lambda_{\Psi h} &= \sqrt{\lambda_S^2 + \lambda_P^2} = \sqrt{\frac{v^2}{\Lambda^2} + \frac{v^2}{\Lambda_5^2}}.\end{aligned}\tag{17}$$

Thus, for different values of $\lambda_P/\lambda_S = \tan \xi$ we may explore $(m_\Psi, \lambda_{\Psi h})$ regions complying with the aforesaid constraints. However, as Λ^{-1} and Λ_5^{-1} belong to the effective operators in Eq. (10), we need to take into account the limited extent of validity of the effective field theory (EFT) approximation. To make a rough estimate for the EFT restraint on $\lambda_{\Psi h}$, we entertain the possibility that each of the operators arises from a tree-level diagram mediated by a heavy scalar X having mass m_X and couplings to Ψ and h described by $\mathcal{L}_X \supset -g_\Psi \bar{\Psi} \Psi X - g_h h^2 X$ in the ultraviolet (UV) completion of the theory. Moreover, inspired by the fermionic and scalar couplings of the SM, we suppose that $g_\Psi \sim \mu_\Psi/v_X$ and $g_h \sim \lambda_{hX} v_X$, where v_X is the VEV of X and λ_{hX} is a constant, ignoring potential modifications due to h - X mixing. The EFT will then remain reliable and perturbative if $1/|\Lambda| \sim 2|\lambda_{hX}|\mu_\Psi/m_X^2 < |\lambda_{hX}|/(2\mu_\Psi) < 2\pi/\mu_\Psi$, as the s -channel $\bar{\Psi}\Psi$ energy \sqrt{s} satisfies $m_X^2 > s > 4\mu_\Psi^2$ and $|\lambda_{hX}| < 4\pi$ for perturbativity.⁴ Similarly, $1/|\Lambda_5| < 2\pi/\mu_\Psi$, although the heavy scalar may be different from X . However, since the preceding bound on λ_{hX} is its most relaxed, it is likely that the EFT breaks down at significantly bigger $|\Lambda|$ and $|\Lambda_5|$, suggesting that it is reasonable to demand instead $|\lambda_{hX}| < \mathcal{O}(1)$. Incorporating these into Eq. (17) and additionally assuming $\mu_\Psi \sim m_\Psi$, we can finally take $\lambda_{\Psi h} < v/m_\Psi$. In the $m_\Psi < m_h/2$ range, this restriction turns out to be much weaker than that from Eq. (15) for the Higgs invisible decay, as will be seen shortly.

Employing Eqs. (12) and (16), we can determine the $\lambda_{\Psi h}$ values consistent with the observed relic density [22] and predict the corresponding Ψ -nucleon cross-section, σ_{el}^N . For a few representative choices of $\tan \xi = \lambda_P/\lambda_S$, we display the results which are depicted by the green curves (labeled 3/2) in Fig. 1. In the left plots, we also draw the upper limits on $\lambda_{\Psi h}$ inferred from Eq. (15) based on the LHC Higgs data [16] (black dotted curves labeled 3/2 as well) and from $\lambda_{\Psi h} < v/m_\Psi$ for the limited validity of the EFT description (magenta dashed curves). The $\lambda_{\Psi h}$ values in the m_Ψ ranges that meet the LHC and EFT requirements in the left plots translate into the solid portions of the green curves for σ_{el}^N in the right plots.

It is evident from graphs (a,c,e,g) in Fig. 1 that as $\lambda_P/\lambda_S = \tan \xi$ exceeds unity the effect of λ_S on the annihilation rate quickly gets negligible, in agreement with expectation, and accordingly the $\lambda_{\Psi h}$ values become independent of this ratio. More interestingly, the instances in Fig. 1 for the spin-3/2 DM illustrate that with $\lambda_P \neq 0$ it is possible to recover at least some of the parameter space excluded by the current direct-search limits in the $\lambda_P = 0$ case, Fig. 1(b), and perhaps even to escape future ones. Especially for $m_\Psi > 50$ GeV, the strictest bound from LUX can be fully evaded if $\lambda_P > 20 \lambda_S$, and the predicted σ_{el}^N over most of this mass region goes below the neutrino-background floor if $\lambda_P > 500 \lambda_S$. However, as graphs (f,h) indicate, for $\lambda_P > 20 \lambda_S$ the LHC and EFT restrictions can be fulfilled only in the range $58 \text{ GeV} \lesssim m_\Psi \lesssim 2.3 \text{ TeV}$.

⁴ The same bound on Λ in the case of spin-1/2 DM was obtained in [4, 6] employing similar arguments.

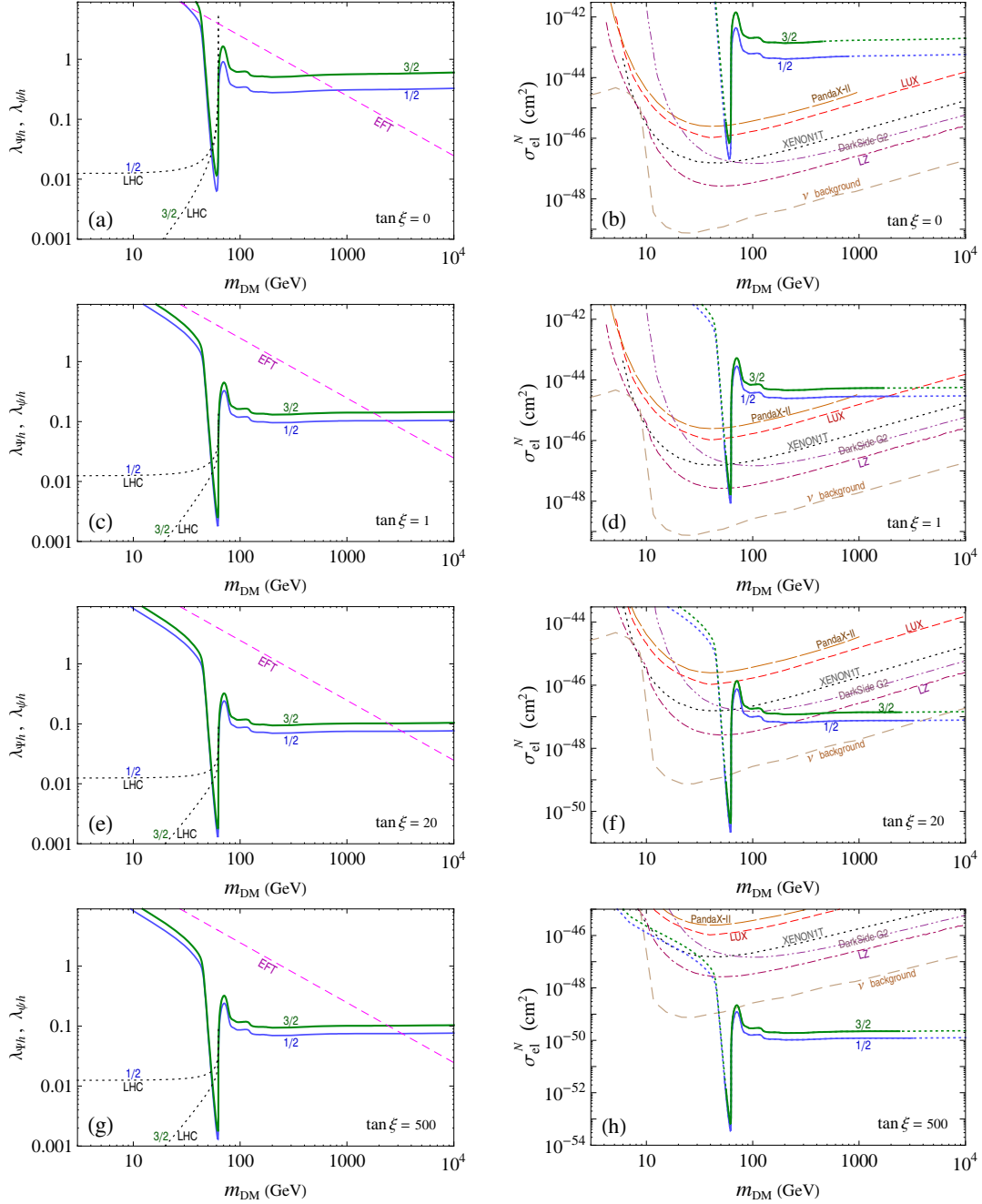


FIG. 1: Left (a,c,e,g): values of the couplings $\lambda_{\psi h}$ and $\lambda_{\psi h}$ of the Higgs to the spin-3/2 DM (green curves) and spin-1/2 DM (blue curves), respectively, versus DM mass which satisfy the relic density requirement for $\tan \xi = 0, 1, 20, 500$, compared to the upper bounds inferred from LHC data on Higgs invisible decay (black dotted curves) and from the limitation of the EFT approach (magenta dashed curves), as described in the text. Right (b,d,f,h): the corresponding DM-nucleon cross-sections σ_{el}^N (green and blue curves), compared to the measured upper-limits from LUX [13] and PandaX-II [14], as well as the sensitivity projections [23] of XENON1T [24], DarkSide G2 [25], and LZ [26], and the WIMP discovery lower-limit due to coherent neutrino scattering backgrounds [27]. The dotted portions of the green and blue curves on the right are excluded by the LHC and EFT restrictions in the left plots.

To provide some further insight into the dependence of σ_{el}^N on $\tan \xi$, we show examples in Fig. 2 for (a) $m_\Psi = 71$, approximately corresponding to the peaks of the green solid curves for σ_{el}^N in Fig. 1, and (b) $m_\Psi = 300$ GeV, which lies in the flat sections of the green curves. From Figs. 1 and 2, we conclude that for $m_\Psi > 300$ GeV and $\tan \xi > 100$ the predicted σ_{el}^N is under the neutrino-background floor.

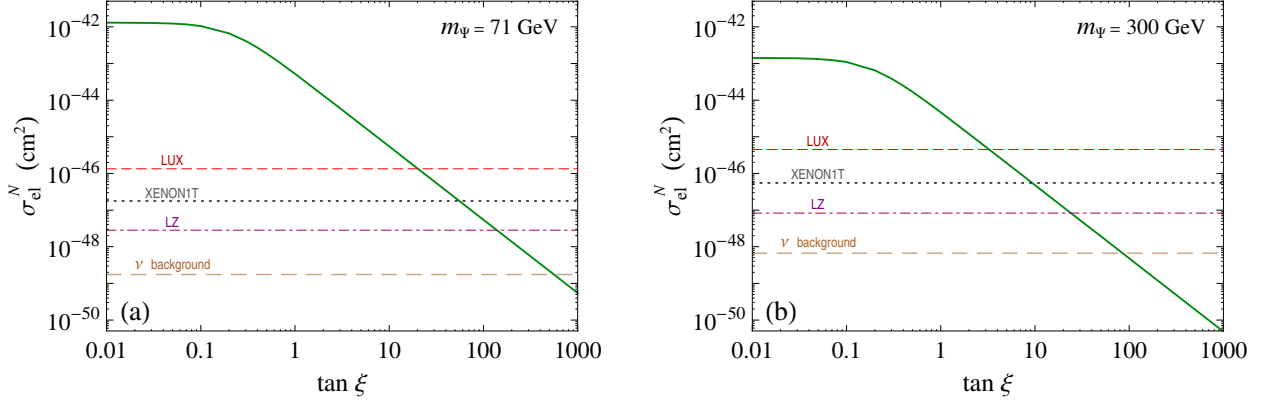


FIG. 2: The Ψ -nucleon cross-sections, σ_{el}^N , (green curves) versus $\tan \xi = \lambda_P / \lambda_S$ for (a) $m_\Psi = 71$ GeV and (b) $m_\Psi = 300$ GeV, compared to the measured upper-limits from LUX [13] as well as the sensitivity projections [23] of XENON1T [24] and LZ [26] and the neutrino background floor [27].

III. COMPARISON WITH HIGGS-PORTAL SPIN-1/2 DM

We expand the SM slightly with the inclusion of a spin-1/2 Dirac field ψ which is a singlet under the SM gauge group and serves as the WIMP DM candidate. It is stable due to the Z_2 symmetry under which only ψ is odd. The DM Lagrangian with leading-order Higgs-portal couplings is then [5–9, 28]

$$\mathcal{L}_\psi = \bar{\psi}(i\not{\partial} - \mu_\psi)\psi - \left(\frac{\bar{\psi}\psi}{\bar{\Lambda}} + \frac{i\bar{\psi}\gamma_5\psi}{\bar{\Lambda}_5} \right) H^\dagger H, \quad (18)$$

where μ_ψ , $\bar{\Lambda}$, and $\bar{\Lambda}_5$ are real constants.⁵ After electroweak symmetry breaking and the transformation of ψ to the mass eigenstate, we have

$$\mathcal{L}_\psi \supset -m_\psi \bar{\psi}\psi - \bar{\psi}(\kappa_S + i\gamma_5 \kappa_P)\psi \left(h + \frac{h^2}{2v} \right), \quad (19)$$

where

$$m_\psi = \sqrt{\left(\mu_\psi + \frac{v^2}{2\bar{\Lambda}} \right)^2 + \frac{v^4}{4\bar{\Lambda}_5^2}}, \quad \kappa_S = \frac{v \cos \bar{\theta}}{\bar{\Lambda}} + \frac{v \sin \bar{\theta}}{\bar{\Lambda}_5}, \quad \kappa_P = \frac{v \cos \bar{\theta}}{\bar{\Lambda}_5} - \frac{v \sin \bar{\theta}}{\bar{\Lambda}},$$

$$\cos \bar{\theta} = \frac{\mu_\psi}{m_\psi} + \frac{v^2}{2\bar{\Lambda}m_\psi}, \quad \sin \bar{\theta} = \frac{v^2}{2\bar{\Lambda}_5m_\psi}. \quad (20)$$

⁵ Some possibilities for the UV completion of this model have been proposed in the literature [28, 29].

We can then derive the cross section σ_{ann} of the DM annihilation given by

$$\begin{aligned}\sigma_{\text{ann}} &= \sigma(\bar{\psi}\psi \rightarrow h^* \rightarrow X_{\text{SM}}) + \sigma(\bar{\psi}\psi \rightarrow hh), \\ \sigma(\bar{\psi}\psi \rightarrow h^* \rightarrow X_{\text{SM}}) &= \frac{(\beta_\psi \kappa_{\text{S}}^2 + \beta_\psi^{-1} \kappa_{\text{P}}^2) \sqrt{s} \sum_i \Gamma(\tilde{h} \rightarrow X_{i,\text{SM}})}{2[(s - m_h^2)^2 + \Gamma_h^2 m_h^2]}, \\ \sigma(\bar{\psi}\psi \rightarrow hh) &= \frac{\beta_h (\beta_\psi \kappa_{\text{S}}^2 + \beta_\psi^{-1} \kappa_{\text{P}}^2)}{64\pi v^2} (\mathcal{R}_{hh}^2 + \mathcal{I}_{hh}^2),\end{aligned}\tag{21}$$

the rate of the invisible decay $h \rightarrow \bar{\psi}\psi$

$$\Gamma(h \rightarrow \bar{\psi}\psi) = \frac{m_h}{8\pi} \left[\kappa_{\text{S}}^2 (1 - 4R_\psi^2)^{3/2} + \kappa_{\text{P}}^2 (1 - 4R_\psi^2)^{1/2} \right],\tag{22}$$

and the cross section of ψ -nucleon elastic scattering

$$\sigma_{\text{el}}^N = \frac{g_{N\psi}^2 m_\psi^2 m_N^2}{\pi (m_\psi + m_N)^2 m_h^4} \left[\kappa_{\text{S}}^2 + \frac{\kappa_{\text{P}}^2 m_N^2 v_{\psi,\text{lab}}^2}{2(m_\psi + m_N)^2} \right],\tag{23}$$

where now $\Gamma_h = \Gamma_h^{\text{SM}} + \Gamma(h \rightarrow \bar{\psi}\psi)$ and $v_{\psi,\text{lab}} = 10^{-3}$. Like in the last section, one notices here that in the nonrelativistic limit the λ_{S} (λ_{P}) part of the annihilation rate (ψ -nucleon cross-section) is substantially suppressed compared to its λ_{P} (λ_{S}) part. This feature of the Higgs-portal spin-1/2 DM is well-known in the literature [5–8, 28].

In Fig. 1 we have also provided examples for $\kappa_{\text{P}}/\kappa_{\text{S}} = \tan \xi = 0, 1, 20, 500$. The blue curves (labeled 1/2) in the left plots represent the values of $\lambda_{\psi h} = (\kappa_{\text{S}}^2 + \kappa_{\text{P}}^2)^{1/2}$ consistent with the observed relic abundance and in the right plots the corresponding predictions for the ψ -nucleon cross-section, σ_{el}^N . Analogously to their spin-3/2 counterparts, the LHC constraint on the Higgs invisible decay implies that $\Gamma(h \rightarrow \bar{\psi}\psi) < 0.16 \Gamma_h$, and the EFT limitation can be expressed as $\lambda_{\psi h} < v/m_\psi$. These are depicted in the left plots by the black dotted curves (labeled 1/2 as well) and the magenta dashed curves, respectively. The $\lambda_{\psi h}$ values in the m_ψ ranges that fulfill these two requirements translate into the solid parts of the blue curves for σ_{el}^N in the right plots. We conclude that for $m_\psi > 50 \text{ GeV}$ and $\kappa_{\text{P}} \gtrsim 20 \kappa_{\text{S}}$ the predicted σ_{el}^N is below all the current bounds from direct searches and may even evade future ones, but the LHC and EFT restraints reduce the allowed mass zone to $54 \text{ GeV} \lesssim m_\psi \lesssim 3.2 \text{ TeV}$.

From the green and blue (solid) curves in Fig. 1, we can make some comparison of these two models. It is obvious that they quite resemble each other phenomenologically, but the viable parameter space of the spin-3/2 DM is somewhat smaller. It follows that new experimental limits on one of the models will likely apply to the other in like manner.

Since there is ample parameter space in these models that can escape upcoming direct searches, even after the LHC and EFT constraints are imposed, it is of interest to consider potential bounds from indirect quests for DM. At present we find a complementary restriction only from the results of searches for DM annihilation signals from the Milky Way dwarf spheroidal galaxies with 6 years of Fermi Large Area Telescope (Fermi-LAT) data [30]. The strongest limit occurs in the $\bar{b}b$ channel, but only for masses between 60 and 70 GeV, as displayed in Fig. 3 for the two models with $\tan \xi = 0, 1, 20$. We expect that improved data in the future from Fermi-LAT [31] as well as the Cherenkov Telescope Array [32] will help probe these models more stringently.

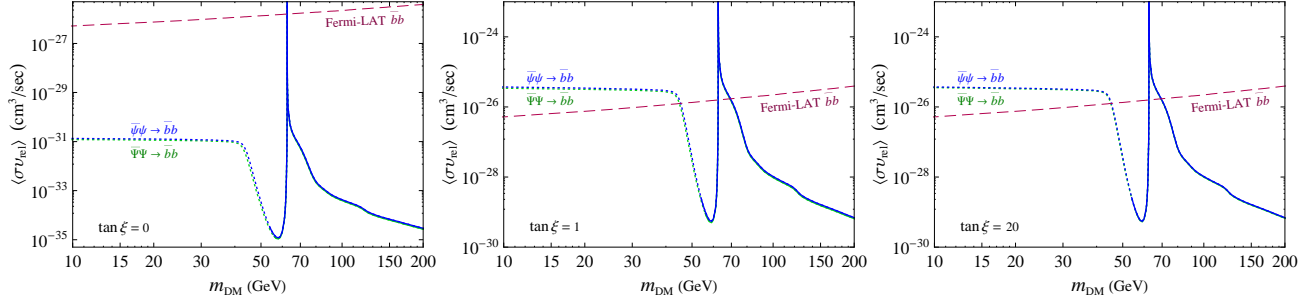


FIG. 3: The thermally averaged annihilation rates of $\bar{\Psi}\Psi \rightarrow \bar{b}b$ and $\bar{\psi}\psi \rightarrow \bar{b}b$ compared to the corresponding Fermi-LAT bound [30].

IV. CONCLUSIONS

We have explored a simple WIMP DM scenario in which the DM candidate has spin 3/2 and Higgs-portal interactions induced by effective dimension-5 scalar and pseudoscalar operators involving the standard Higgs doublet. Our examples illustrate that the inclusion of the pseudoscalar operator in addition to the scalar one is crucial for the model to avoid the existing strong restrictions from direct detection experiments and also to evade future ones. We also implement the restraints from Higgs data and EFT considerations, which decrease the allowed DM-mass region to between 58 GeV and 2.3 TeV. We obtain an extra constraint from indirect searches by Fermi-LAT which disfavors masses between 60 and 70 GeV. Finally, we show that this model is similar in many ways to its spin-1/2 counterpart, but has viable parameter space that is slightly more reduced. Therefore, the combination of future data from LHC measurements and DM (in)direct searches can be expected to test these two models more comprehensively.

Acknowledgments

This work was supported in part by MOE Academic Excellence Program (Grant No. 105R891505) and NCTS of ROC. X.-G. He was also supported in part by MOST of ROC (Grant No. MOST104-2112-M-002-015-MY3) and in part by NSFC (Grant Nos. 11175115 and 11575111), Key Laboratory for Particle Physics, Astrophysics and Cosmology, Ministry of Education, and Shanghai Key Laboratory for Particle Physics and Cosmology (SKLPPC) (Grant No. 11DZ2260700) of PRC.

-
- [1] C. Patrignani *et al.* [Particle Data Group], Chin. Phys. C **40**, no. 10, 100001 (2016).
 - [2] S. Baek, P. Ko, and W.I. Park, Phys. Rev. D **90**, no. 5, 055014 (2014) [arXiv:1405.3530 [hep-ph]].
 - [3] X.G. He and J. Tandean, JHEP **1612**, 074 (2016) [arXiv:1609.03551 [hep-ph]].
 - [4] G. Busoni, A. De Simone, J. Gramling, E. Morgante, and A. Riotto, JCAP **1406**, 060 (2014) [arXiv:1402.1275 [hep-ph]].

- [5] M.A. Fedderke, J.Y. Chen, E.W. Kolb, and L.T. Wang, JHEP **1408**, 122 (2014) [arXiv:1404.2283 [hep-ph]].
- [6] A. Beniwal, F. Rajec, C. Savage, P. Scott, C. Weniger, M. White, and A.G. Williams, Phys. Rev. D **93**, no. 11, 115016 (2016) [arXiv:1512.06458 [hep-ph]].
- [7] M. Escudero, A. Berlin, D. Hooper, and M.X. Lin, JCAP **1612**, no. 12, 029 (2016) [arXiv:1609.09079 [hep-ph]].
- [8] G. Arcadi, M. Dutra, P. Ghosh, M. Lindner, Y. Mambrini, M. Pierre, S. Profumo, and F.S. Queiroz, arXiv:1703.07364 [hep-ph].
- [9] J.F. Kamenik and C. Smith, JHEP **1203**, 090 (2012) [arXiv:1111.6402 [hep-ph]]; Phys. Rev. D **85**, 093017 (2012) [arXiv:1201.4814 [hep-ph]].
- [10] Z.H. Yu, J.M. Zheng, X.J. Bi, Z. Li, D.X. Yao, and H. H. Zhang, Nucl. Phys. B **860**, 115 (2012) [arXiv:1112.6052 [hep-ph]]; R. Ding and Y. Liao, JHEP **1204**, 054 (2012) [arXiv:1201.0506 [hep-ph]]; R. Ding, Y. Liao, J.Y. Liu, and K. Wang, JCAP **1305**, 028 (2013) [arXiv:1302.4034 [hep-ph]]; S. Dutta, A. Goyal, and S. Kumar, JCAP **1602**, no. 02, 016 (2016) [arXiv:1509.02105 [hep-ph]].
- [11] C.F. Chang, X.G. He, and J. Tandean, arXiv:1702.02924 [hep-ph].
- [12] K.G. Savvidy and J.D. Vergados, Phys. Rev. D **87**, no. 7, 075013 (2013) [arXiv:1211.3214 [hep-ph]]; L. Roszkowski, S. Trojanowski, K. Turzynski, and K. Jedamzik, JHEP **1303**, 013 (2013) [arXiv:1212.5587 [hep-ph]]; J. Hasenkamp and M.W. Winkler, Nucl. Phys. B **877**, 419 (2013) [arXiv:1308.2678 [hep-ph]]; M.O. Khojali, A. Goyal, M. Kumar, and A.S. Cornell, Eur. Phys. J. C **77**, no. 1, 25 (2017) [arXiv:1608.08958 [hep-ph]].
- [13] D.S. Akerib *et al.*, arXiv:1608.07648 [astro-ph.CO].
- [14] A. Tan *et al.* [PandaX-II Collaboration], Phys. Rev. Lett. **117**, no. 12, 121303 (2016) [arXiv:1607.07400 [hep-ex]].
- [15] G. Aad *et al.* [ATLAS Collaboration], JHEP **1511**, 206 (2015) [arXiv:1509.00672 [hep-ex]]. V. Khachatryan *et al.* [CMS Collaboration], [arXiv:1610.09218 [hep-ex]].
- [16] The ATLAS and CMS Collaborations, JHEP **1608**, 045 (2016) [arXiv:1606.02266 [hep-ex]].
- [17] W. Rarita and J. Schwinger, Phys. Rev. **60**, 61 (1941).
- [18] P.A. Moldauer and K.M. Case, Phys. Rev. **102**, 279 (1956); C. Fronsdaal, Nuovo Cimento Suppl. **9**, 416 (1958).
- [19] N.D. Christensen *et al.*, Eur. Phys. J. C **73**, no. 10, 2580 (2013) [arXiv:1308.1668 [hep-ph]].
- [20] G. Aad *et al.* [ATLAS and CMS Collaborations], Phys. Rev. Lett. **114**, 191803 (2015) [arXiv:1503.07589 [hep-ex]].
- [21] S. Heinemeyer *et al.* [LHC Higgs Cross Section Working Group Collaboration], arXiv:1307.1347 [hep-ph]. Online updates available at <https://twiki.cern.ch/twiki/bin/view/LHCPhysics/CERNYellowReportPageBR2014>.
- [22] P.A.R. Ade *et al.* [Planck Collaboration], Astron. Astrophys. **594**, A13 (2016) [arXiv:1502.01589 [astro-ph.CO]].
- [23] P. Cushman *et al.*, arXiv:1310.8327 [hep-ex].
- [24] E. Aprile *et al.* [XENON Collaboration], JCAP **1604**, no. 04, 027 (2016) [arXiv:1512.07501 [physics.ins-det]].
- [25] C.E. Aalseth *et al.*, Adv. High Energy Phys. **2015**, 541362 (2015). doi:10.1155/2015/541362
- [26] D.S. Akerib *et al.* [LZ Collaboration], arXiv:1509.02910 [physics.ins-det].
- [27] J. Billard, L. Strigari, and E. Figueroa-Feliciano, Phys. Rev. D **89**, no. 2, 023524 (2014) [arXiv:1307.5458 [hep-ph]].
- [28] L. Lopez-Honorez, T. Schwetz, and J. Zupan, Phys. Lett. B **716**, 179 (2012) [arXiv:1203.2064 [hep-ph]].

- [29] H.C. Tsai and K.C. Yang, Phys. Rev. D **87**, no. 11, 115016 (2013) [arXiv:1301.4186 [hep-ph]]; K. Ghorbani, JCAP **1501**, 015 (2015) [arXiv:1408.4929 [hep-ph]]; Y.G. Kim, K.Y. Lee, C.B. Park, and S. Shin, Phys. Rev. D **93**, no. 7, 075023 (2016) [arXiv:1601.05089 [hep-ph]]; S. Baek, P. Ko, and J. Li, arXiv:1701.04131 [hep-ph].
- [30] M. Ackermann *et al.* [Fermi-LAT Collaboration], Phys. Rev. Lett. **115**, no. 23, 231301 (2015) [arXiv:1503.02641 [astro-ph.HE]].
- [31] E. Charles *et al.* [Fermi-LAT Collaboration], Phys. Rept. **636**, 1 (2016) [arXiv:1605.02016 [astro-ph.HE]].
- [32] M. Doro *et al.* [CTA Consortium], Astropart. Phys. **43**, 189 (2013) [arXiv:1208.5356 [astro-ph.IM]].